Surendar et al. *Boundary Value Problems* (2023) 2023:81
https://doi.org/10.1186/s13661-023-01771-w

Boundary Value Problems
a SpringerOpen Journal

RESEARCH Open Access

Qualitative analysis of a prey–predator model with prey refuge and intraspecific competition among predators

Maruthai Selvaraj Surendar[1], Muniagounder Sambath[2], Krishnan Balachandran[3] and Yong-Ki Ma[4*]

*Correspondence: ykma@kongju.ac.kr
[4]Department of Applied Mathematics, Kongju National University, Gongju-si, Chungcheongnam-do 32588, Republic of Korea
Full list of author information is available at the end of the article

Abstract

In this study, we consider a prey–predator model with prey refuge and intraspecific competition between predators using the Crowley–Martin functional response and investigate the dynamic characteristics of spatial and nonspatial prey–predator systems via both analytical and numerical methods. The local stability of nontrivial interior equilibrium, the existence of a Hopf bifurcation, and the stability of bifurcating periodic solutions are obtained in the absence of diffusion. For the spatial system, the Turing and non-Turing patterns are evaluated for some set of parametric belief functions, and we obtain some interesting results in terms of prey and predator inhabitants. We present the results of numerical simulations that demonstrate that both prey and predator populations do not converge to a stationary equilibrium state at any foreseeable future time when the parametric values are processed in the Turing domain.

Mathematics Subject Classification: 35K57; 92D25; 70K50; 34D20

Keywords: Stability analysis; Prey–predator model; Refuge; Hopf bifurcation; Crowley–Martin functional response; Turing instability

1 Introduction

Understanding the dynamics of interacting prey–predator models is of paramount importance for gaining insights into the long-term behavior of species in ecological systems. Over the years, researchers have extensively investigated various nonlinear coupled ordinary differential equations to model the complex interactions among prey and their potential predators. Among the classical models, the Lotka–Volterra model, introduced independently by Lotka and Volterra in the early twentieth century, has served as a fundamental basis for studying predator–prey interactions. Subsequent advancements by Holling [18] in the form of the Rosenzweig–MacArthur model [33] incorporated density-dependent prey growth and functional response.

While these classical models have provided valuable insights into the general characteristics of prey–predator populations, recent research has shown that incorporating additional factors can better reflect the intricacies of natural ecosystems. Consequently, researchers have introduced various functional responses to represent the feeding rates of

© The Author(s) 2023. **Open Access** This article is licensed under a Creative Commons Attribution 4.0 International License, which permits use, sharing, adaptation, distribution and reproduction in any medium or format, as long as you give appropriate credit to the original author(s) and the source, provide a link to the Creative Commons licence, and indicate if changes were made. The images or other third party material in this article are included in the article's Creative Commons licence, unless indicated otherwise in a credit line to the material. If material is not included in the article's Creative Commons licence and your intended use is not permitted by statutory regulation or exceeds the permitted use, you will need to obtain permission directly from the copyright holder. To view a copy of this licence, visit http://creativecommons.org/licenses/by/4.0/.

predators [5, 49, 50]. Notably, the Lotka–Volterra and Holling types have been widely used in this context.

Additionally, the most crucial concept in prey–predator models is the 'functional response', which describes the rate at which a predator attacks a given number of prey. The Lotka–Volterra and Holling types are the most commonly used functional responses to represent the average feeding rate of a predator.

$$\begin{aligned}
&\text{Lotka–Volterra type}: \quad f_1(u) = \delta u,\\
&\text{Holling Type-II}: \quad f_2(u) = \delta u/(1+\alpha u),\\
&\text{Holling Type-III}: \quad f_3(u) = \delta u^2/\bigl(1+\alpha u^2\bigr),\\
&\text{Holling Type-IV}: \quad f_4(u) = \delta u/\bigl(1+\alpha u^2\bigr),
\end{aligned}$$

where u denotes the density of the prey population, and δ and α are positive constants that respectively represent the effects of capture rate and handling time. Notably, these four functional response features are prey-dependent and generally not influenced by predator inhabitants. However, a crucial aspect often overlooked in these models is the consideration of mutual interference among potential predators. To address this limitation, Beddington [2] and DeAngelis [11] proposed a functional response

$$f(u,v) = \delta u/(1+\alpha u+\beta v)$$

that accounts for predator (v) interference β, while Crowley and Martin [10] introduced a similar response, taking into account both searching and handling interference:

$$f(u,v) = \delta u/\bigl((1+\alpha u)(1+\beta v)\bigr),$$

which is referred to as the Crowley–Martin functional response. These modifications have proven essential in understanding the dynamics of real-world predator–prey systems, and they offer a more accurate representation of their behavior [38].

In recent years, the study of prey–predator models has witnessed significant developments, with researchers incorporating various factors such as the Allee effect, prey refuge, interference among predators, and harvesting [6, 15, 25–27, 29, 36, 37, 47, 48]. These enhancements have allowed for a more detailed reflection of the behavior of natural ecosystems, leading to a growing interest in the dynamic characteristics of these models [3, 4, 7, 8, 14, 19, 20, 22–24, 30, 31, 35, 39–46].

In light of these considerations, the present study focuses on formulating a prey–predator model that accounts for prey refuge and intraspecific competition among predators using the Crowley–Martin functional response. The inclusion of prey refuge and competition among predators in the model is crucial as it addresses important ecological aspects that have significant implications for species coexistence and ecosystem stability.

The rest of this paper is organized as follows: Sect. 2 presents the mathematical formulation of the prey–predator model with prey refuge and intraspecific competition among predators using the Crowley–Martin functional response. In Sect. 3, we analyze the existence and local and global dynamics of equilibria. Subsequently, in Sect. 4, we discuss the presence of Hopf bifurcation and its periodic solution behaviors. Section 5 focuses

on the occurrence of Turing instability in the interior equilibrium point under the influence of diffusion. Theoretical results are verified through numerical simulations in Sect. 6, where we also uncover additional meaningful phenomena. Finally, Sect. 7 offers concluding remarks and highlights the significance of our findings within the broader context of ecological research.

By comprehensively investigating the dynamic behavior of this extended prey–predator model, we aim to contribute to a deeper understanding of ecological interactions and enhance the applicability of predator–prey models in real-world scenarios.

2 Mathematical model and analysis

Bazykin [1] introduced a prey–predator model based on the Crowley–Martin (C-M) functional response, which considers the simultaneous involvement of potential predators in various activities, including searching and handling prey as well as interacting with other predators. The C-M functional response is described by the total instantaneous per capita feeding rate equation

$$f(X,Y) := \frac{\tilde{a}XY}{1+\tilde{b}X+\tilde{c}(Y-1)}.$$

Here, X denotes the prey population, Y denotes the predator population, and $\tilde{c}$ (units: 1/predator) represents the magnitude of interference among predators. The term $Y-1$ is used to account for the mechanistic nature of predator dependence, indicating that a predator does not interfere with itself in these models. When $Y=1$, the equation reduces to the traditional Holling Type II response.

Prey refuge, a significant concept in prey–predator models, plays a crucial role in supporting a constant proportion of prey through predation [16, 17]. It profoundly influences the coexistence of predators and prey. In theoretical ecology, understanding the impact of prey refuge on the dynamics of prey–predator interactions has been a topic of interest. Many authors [9, 12, 21, 34] have found that prey refuge stabilizes prey–predator dynamics, preserving prey biomass and preventing extinction due to predation. Therefore, the strength of prey refuges affects the foraging efficiency of predators.

To incorporate the effect of prey refuge, we integrate it into the C-M functional response term. As a result, we arrive at the nonautonomous C-M type prey–predator model, accounting for prey refuge and intraspecific competition among predators for prey:

$$\begin{cases} \frac{dX(t)}{dt} = X(r_1-\rho X) - \frac{\delta_1(1-m)XY}{\chi_1+\chi_2(1-m)X+\chi_3((1-m)X)(Y-1)}, \\ \frac{dY(t)}{dt} = r_2Y - \frac{\delta_2Y^2}{\chi_4+(1-m)X} - \delta_3Y, \\ X(0)=X_0>0, \qquad Y(0)=Y_0>0. \end{cases} \tag{2.1}$$

In this model, $X(t)$ represents the biomass of the prey population, and $Y(t)$ denotes the biomass of the predator population at time t. The refuge protects a population of prey denoted by mX, where $m \in [0,1)$ is a constant, making $(1-m)X$ the only prey available to predators. The parameters r_1, r_2, ρ, δ_1, δ_2, δ_3, χ_1, χ_2, χ_3, and χ_4 are all positive constants with ecological meaning as follows in Table 1.

Assuming a biological perspective, we confirm that $\chi_1+\chi_2(1-m)X+\chi_3((1-m)X)(Y-1) \neq 0$, ensuring the well-posedness of our system (2.1).

Table 1 Ecological meaning

Parameter	Biological/ecological meaning
r_1	Growth rate of prey population in the absence of predators,
r_2	Growth rate of predators (based on the convention coefficients from prey individuals to predator individuals),
ρ	Strength of competition among individuals of prey species,
δ_1	Maximum value of per capita reduction rate of prey,
δ_2	Maximum value of per capita predator consumption rate,
δ_3	Death rate of predators,
χ_1	Half saturation constant of prey in absence of refuge,
χ_2	Measures the handling time of prey on the feeding rate,
χ_3	Coefficient of interference (disturbance) among predators,
χ_4	Measures the extent to which the environment provides protection to a predator.

For simplicity, we proceed to nondimensionalize (2.1) using the following scaling:

$$u \mapsto \rho X, \qquad v \mapsto Y, \qquad t \mapsto t.$$

This leads us to the following form of the model:

$$\begin{cases} \dot{u}(t) = u(r-u) - \frac{\delta(1-m)uv}{1+\alpha(1-m)u+\beta((1-m)u)(v-1)}, \\ \dot{v}(t) = \xi(\zeta v - \frac{v^2}{\eta+(1-m)u} - \sigma v), \\ u(0) = u_0 > 0, \qquad v(0) = v_0 > 0. \end{cases} \tag{2.2}$$

In this formulation, we define dimensionless constants as follows: $r = r_1$, $\delta = \frac{\delta_1}{\chi_1}$, $\alpha = \frac{\chi_2}{\rho\chi_1}$, $\beta = \frac{\chi_3}{\rho\chi_1}$, $\xi = \frac{\delta_2}{\rho}$, $\zeta = \frac{r_2\rho}{\delta_2}$, $\eta = \rho\chi_4$, and $\sigma = \frac{\delta_3\rho}{\delta_2}$.

Our physical world exists within a spatial universe, where environmental interactions play a vital role in shaping ecological communities. Various aspects, such as the atmosphere, geological materials, and biological frameworks, differ significantly across the planet. Consequently, population dynamics depend on both space and time, incorporating spatial movement. To analyze the spatial dynamics of prey–predator models, we consider the following system of partial differential equations with homogeneous Neumann boundary conditions:

$$\begin{cases} \frac{\partial u(x,t)}{\partial t} = u(r-u) - \frac{\delta(1-m)uv}{1+\alpha(1-m)u+\beta((1-m)u)(v-1)} + D_1\nabla^2 u, \quad x \in \Omega, t > 0, \\ \frac{\partial v(x,t)}{\partial t} = \xi(\zeta v - \frac{v^2}{\eta+(1-m)u} - \sigma v) + D_2\nabla^2 v, \quad x \in \Omega, t > 0, \\ \partial_\nu u = \partial_\nu v = 0, \quad x \in \partial\Omega, t > 0, \\ u(x,0) = u_0(x) \geq 0, \qquad v(x,0) = v_0(x) \geq 0, \quad x \in \Omega. \end{cases} \tag{2.3}$$

In this spatial extension, $u(x,t)$ and $v(x,t)$ represent the densities of prey and predators, respectively, in the fixed open bounded domain $\Omega \subset \mathbb{R}^N$ at time t. The diffusion coefficients D_1 and D_2 account for the spatial movement of prey and predators, respectively. The Laplacian operator $\nabla^2 = \frac{\partial^2}{\partial u^2} + \frac{\partial^2}{\partial v^2}$ describes spatial interactions in a two-dimensional space.

The boundary $\partial\Omega$ of the domain Ω is smooth, and ν represents the outward unit normal vector of the boundary. The homogeneous Neumann boundary conditions indicate that the prey–predator system is self-contained with no population flux across the boundary.

3 Equilibrium points and stability analysis

3.1 Equilibria

System (2.2) has trivial and axial equilibrium points where E_0, E_1, E_2 always exist, where the following occur:

(i) Trivial equilibrium point: $E_0 = (0,0)$, both prey and predator are extinct.

(ii) Axial equilibrium points: $E_1 = (r,0)$, only prey survives; $E_2 = (0, \zeta\eta - \eta\sigma)$, if $\zeta > \sigma$, only predators survive.

The nontrivial interior equilibrium point $E^*(u^*, v^*) \in \mathbb{R}^2_+$ can be obtained by solving the following system of equations:

$$u(r-u) - \frac{\delta(1-m)uv}{1+\alpha(1-m)u+\beta((1-m)u)(v-1)} = 0,$$
$$\xi\left(\zeta v - \frac{v^2}{\eta+(1-m)u} - \sigma v\right) = 0.$$

Solving these nullclines, we obtain a cubic equation in u:

$$\Delta_1 u^3 + \Delta_2 u^2 + \Delta_3 u + \Delta_4 = 0, \tag{3.1}$$

where (H): $\Delta_1 = -(m-1)^2\beta(\zeta-\sigma) < 0$, $\Delta_2 = (m-1)(\alpha+\beta(-1+((m-1)r+\eta)(\zeta-\sigma))) < 0$, $\Delta_3 = -1-(m-1)^2\delta(\zeta-\sigma)-(m-1)r(\alpha+\beta(-1+\eta(\zeta-\sigma))) > 0$, $\Delta_4 = r+(m-1)\delta\eta(\zeta-\sigma) > 0$, provided the cubic equation (3.1) has at most one positive solution u^* (say). Using the value of u^*, we obtain the value of v^* as follows:

$$v^* = (\zeta-\sigma)\big(\eta+(1-m)u^*\big),$$

$\zeta > \sigma$ provided v^* is also positive.

Below we assume that all $E^*(u^*, v^*)$ ensure the above conditions (H) and $\zeta > \sigma$.

3.2 Local stability analysis

The dynamic behavior of the equilibrium points can be studied by computing the eigenvalues of the Jacobian matrix J of system (2.2), namely,

$$J = \begin{pmatrix} r-2u-\frac{\delta(1-m)v}{((m-1)u(\alpha+(v-1)\beta)-1)^2} & \frac{\delta(1-m)(-1+(m-1)u(\alpha-\beta))u}{((m-1)u(\alpha+(v-1)\beta)-1)^2} \\ \frac{-\xi(m-1)v^2}{(\eta+(1-m)u)^2} & \xi(\zeta-\frac{2v}{\eta+(1-m)u}-\sigma) \end{pmatrix}. \tag{3.2}$$

The existence and local stability of the equilibrium solutions can be stated as follows.

Theorem 3.1

(i) *The trivial equilibrium point $E_0 = (0,0)$ is always unstable.*

(ii) *If $\zeta < \sigma$, then the axial equilibrium point $E_1 = (r,0)$ is locally asymptotically stable.*

(iii) *The axial equilibrium point $E_2 = (0, \eta(\zeta-\sigma))$ is always unstable.*

Proof (i) The Jacobian matrix of system (2.2) evaluated at the equilibrium point $E_0 = (0,0)$ is given by

$$J|_{E_0} = \begin{pmatrix} r & 0 \\ 0 & \xi(\zeta-\sigma) \end{pmatrix},$$

$\operatorname{tr} J|_{E_0} = r + \xi(\zeta - \sigma)$ and $\det J|_{E_0} = r\xi(\zeta - \sigma)$. The eigenvalues corresponding to $J|_{E_0}$ are $\lambda_1 = r\ (>0)$ and $\lambda_2 = \xi(\zeta - \sigma)$. Thus E_0 is unstable when $\zeta > \sigma$ $(\lambda_2 > 0)$, and E_0 is a saddle point when $\zeta < \sigma$ $(\lambda_2 < 0)$. Therefore, $E_0 = (0,0)$ is always unstable.

(ii) The Jacobian matrix of system (2.2) evaluated at the axial equilibrium point $E_1 = (r,0)$ is given by

$$J|_{E_1} = \begin{pmatrix} -r & \frac{-(m-1)r\delta}{(m-1)(\alpha-\beta)r-1} \\ 0 & \xi(\zeta - \sigma) \end{pmatrix},$$

$\operatorname{tr} J|_{E_1} = -r + \xi(\zeta - \sigma)$ and $\det J|_{E_1} = -r\xi(\zeta - \sigma)$. When $\zeta < \sigma$, $\det J|_{E_1} > 0$ and $\operatorname{tr} J|_{E_1} < 0$. Therefore, E_1 is locally asymptotically stable when $\zeta < \sigma$.

(iii) The Jacobian matrix of system (2.2) evaluated at the axial equilibrium point $E_2 = (0, \eta(\zeta - \sigma))$ is given by

$$J|_{E_2} = \begin{pmatrix} r + \delta\eta(m-1)(\zeta - \sigma) & 0 \\ -\xi(m-1)(\zeta - \sigma)^2 & -\xi(\zeta - \sigma) \end{pmatrix}.$$

Then the eigenvalues of the above Jacobi matrix $J|_{E_2}$ are $\mu_1 = r + \delta\eta(1-m)(\zeta - \sigma)$ and $\mu_2 = -\xi(\zeta - \sigma)$. When $\zeta < \sigma$ $(\mu_2 < 0)$ and $r < \delta\eta(1-m)(\zeta - \sigma)$ $(\mu_1 < 0)$, both eigenvalues are negative. Hence, the axial equilibrium point E_2 is locally asymptotically stable when $\zeta < \sigma$ and $r < \delta\eta(1-m)(\zeta - \sigma)$. This is not possible because $\zeta < \sigma \implies \delta\eta(1-m)(\zeta - \sigma) < 0$ and because of our assumption that $r > 0$. This shows that the locally asymptotically stable situation never occurs. Therefore, E_2 is always unstable. Also note that $\zeta < \sigma \implies E_2 < 0$ (i.e., when $E_2 \notin \{\{0\} \cup \mathbb{R}\}_+^2$, the predators also die out). □

3.3 Interior equilibrium qualitative behaviors

The Jacobian matrix evaluated at the coexistence equilibrium point $E^*(u^*, v^*)$ is

$$J|_{E^*} = \begin{pmatrix} a_{11} & a_{12} \\ a_{21} & a_{22} \end{pmatrix}, \tag{3.3}$$

where $a_{11} = r - 2u^* - \frac{\delta(1-m)v^*}{((m-1)u^*(\alpha+(v^*-1)\beta)-1)^2}$, $a_{12} = \frac{\delta(1-m)(-1+(m-1)u^*(\alpha-\beta))u^*}{((m-1)u^*(\alpha+(v^*-1)\beta)-1)^2}$, $a_{21} = \frac{-\xi(m-1)v^{*2}}{(\eta+(1-m)u^*)^2}$, $a_{22} = \xi(\zeta - \frac{2v^*}{\eta+(1-m)u^*} - \sigma)$.

Then the trace and determinant of the Jacobian matrix (3.3) is

$$T = \operatorname{tr} J|_{E^*} = a_{11} + a_{22} \quad \text{and} \quad D = \det J|_{E^*} = a_{11}a_{22} - a_{21}a_{12}.$$

Therefore, the characteristic equation of the linearized system of (2.2) at $E^* = (u^*, v^*)$ is

$$\lambda^2 - T\lambda + D = 0. \tag{3.4}$$

The qualitative behaviors of the interior equilibrium point $E^*(u^*, v^*)$ may be stated as follows.

Case (i): If $T < 0$ and $D > 0$, then the characteristic roots of (3.4) are either both negative reals or complex conjugates with a negative real part. Therefore, E^* is either a stable node ($T^2 > 4D$) or a stable spiral ($T^2 < 4D$).

Case (ii): If $T > 0$ and $D > 0$, then the characteristic roots of (3.4) are either both positive reals or complex conjugates with a positive real part. Hence, E^* is either an unstable node ($T^2 > 4D$) or an unstable spiral ($T^2 < 4D$).

Case (iii): If $D < 0$ and $T \neq 0$, then the characteristic roots of (3.4) are both are real with opposite signs. Therefore E^* is a saddle point.

Case (iv): If $D < 0$ and $T = 0$, then the characteristic roots of (3.4) both are real numbers with same magnitude and opposite signs. Hence, E^* is a saddle node.

Case (v): If $D > 0$ and $T = 0$, then the characteristic roots of (3.4) are purely complex conjugate. Therefore, E^* is a center.

3.4 Global stability analysis

Here, we provide the result to attain global stability in the nontrivial interior equilibrium $E^* = (u^*, v^*)$ for both local (2.2) and spatial (2.3) systems.

Theorem 3.2 *If* $(\delta(1-m)v^* - u^*)\alpha < \frac{1}{1-m} + \beta u^*(v^* - 1)$ *and* $(1-m)u^*(\beta - \alpha) < 1$ *hold, then the interior equilibrium* $E^* = (u^*, v^*)$ *of the local system* (2.2) *is globally asymptotically stable.*

Proof The proof is usually developed by applying the Lyapunov function. We consider the subsequent positive definite Lyapunov function in $\mathbb{R}$ about the equilibrium E^*:

$$V_1 = u - u^* - u^* \ln\left(\frac{u}{u^*}\right) \quad \text{and}$$
$$V_2 = v - v^* - v^* \ln\left(\frac{v}{v^*}\right).$$

This kind of Lyapunov function was first utilized in [13], and later it was broadly exploited by several researchers. We can simply verify that $\frac{\partial V_1}{\partial u} > 0$ for $u > u^*$ and $\frac{\partial V_1}{\partial u} < 0$ for $0 < u < u^*$, and $\frac{\partial V_2}{\partial v} > 0$ for $v > v^*$ and $\frac{\partial V_2}{\partial v} < 0$ for $0 < v < v^*$. If we estimate $\frac{\partial V_1}{\partial t}$ via (2.2), we obtain

$$\begin{aligned}
\frac{dV_1(u)}{dt} &= \left(u - u^*\right)\frac{\dot{u}}{u} = \left(1 - \frac{u^*}{u}\right)\left\{u(r-u) - \frac{\delta(1-m)uv}{\Theta}\right\}, \\
&= \left(u - u^*\right)\left\{-\left(u - u^*\right) - \left(\frac{\delta(1-m)v}{\Theta} - \frac{\delta(1-m)v^*}{\widehat{\Theta}}\right)\right\}, \\
&= \left(u - u^*\right)^2\left\{\frac{\delta(1-m)(\alpha(1-m)v^* - \beta(1-m)v^*(1-v))}{\Theta\widehat{\Theta}} - 1\right\} \\
&\quad - \frac{\delta(1-m)(1 + \alpha(1-m)u^* - \beta(1-m)u^*)(u-u^*)(v-v^*)}{\Theta\widehat{\Theta}},
\end{aligned} \tag{3.5}$$

where $\Theta = 1 + \alpha(1-m)u + \beta((1-m)u)(v-1)$, $\widehat{\Theta} = 1 + \alpha(1-m)u^* + \beta((1-m)u^*)(v^*-1)$.

Similarly,

$$\begin{aligned}
\frac{dV_2(v)}{dt} &= \left(v - v^*\right)\frac{\dot{v}}{v} = \left(1 - \frac{v^*}{v}\right)\left\{\xi\left(\zeta v - \frac{v^2}{\Phi} - \sigma v\right)\right\}, = \left(v - v^*\right)\left\{\frac{-\xi v}{\Phi} + \frac{\xi v^*}{\widehat{\Phi}}\right\}, \\
&= \frac{-\xi(v-v^*)^2}{\Phi} + \frac{\xi(1-m)v^*(u-u^*)(v-v^*)}{\Phi\widehat{\Phi}},
\end{aligned} \tag{3.6}$$

where $\Phi = \eta + (1-m)u$, $\widehat{\Phi} = \eta + (1-m)u^*$.

We define the Lyapunov function $V = V_1(u) + \frac{1}{C}V_2(v)$, where $C = \frac{\xi v^*}{\delta(1+\alpha(1-m)u^*-\beta(1-m)u^*)}$. Generating $\frac{dV}{dt}$ via (3.5) and (3.6) gives

$$\begin{aligned}\frac{dV}{dt} &= \left(u-u^*\right)^2\left\{\frac{\delta(1-m)(1+\alpha(1-m)u^*-\beta(1-m)v^*(1-v))}{\Theta\widehat{\Theta}}-1\right\}\\ &\quad-\left(v-v^*\right)^2\left\{\frac{\delta(1+\alpha(1-m)u^*-\beta(1-m)u^*)}{v^*\Phi}\right\}.\end{aligned} \tag{3.7}$$

The coefficient of $(u-u^*)^2$ is

$$\begin{aligned}&\frac{\delta(1-m)(1+\alpha(1-m)u^*-\beta(1-m)v^*(1-v))}{\Theta\widehat{\Theta}}-1\\ &\quad\le\frac{\delta(1-m)(1+\alpha(1-m)u^*-\beta(1-m)v^*(1-v))}{\widehat{\Theta}}-1.\end{aligned}$$

The coefficient of $(v-v^*)^2$ is

$$-\frac{\delta(1+\alpha(1-m)u^*-\beta(1-m)u^*)}{v^*\Phi}\le-\frac{\delta(1+\alpha(1-m)u^*-\beta(1-m)u^*)}{v^*}.$$

Therefore, if $(\delta(1-m)v^*-u^*)\alpha<\frac{1}{1-m}+\beta u^*(v^*-1)$ and $(1-m)u^*(\beta-\alpha)<1$ hold consequently from (3.7), then we obtain $\frac{dV}{dt}<0$. Hence, by Lyapunov's asymptotic stability theorem, the interior equilibrium E^* of system (2.2) is globally asymptotically stable. □

Now, we select the Lyapunov function for the diffusion system (2.3)

$$E(t)=\iint_\Omega V(u,v)\,dA. \tag{3.8}$$

Hence, differentiating $E(t)$ with respect to t along the solutions of system (2.3), we obtain

$$\frac{dE(t)}{dt}=\iint_\Omega\left(\frac{\partial V}{\partial u}d_1\nabla^2u+\frac{\partial V}{\partial v}d_2\nabla^2v\right)dA+\iint_\Omega\frac{dV}{dt}\,dA.$$

Considering the zero-flux boundary conditions $\partial_\nu u=\partial_\nu v=0$, $x\in\partial\Omega$ and applying Green's first identity in the plane, we obtain

$$\begin{aligned}\frac{dE(t)}{dt}&=\iint_\Omega\frac{dV}{dt}\,dA-\left\{\frac{d_1u^*}{u^2}\iint_\Omega\left(\left(\frac{\partial u}{\partial x}\right)^2+\left(\frac{\partial u}{\partial y}\right)^2\right)dA\right.\\ &\quad\left.+\frac{d_2v^*}{v^2}\iint_\Omega\left(\left(\frac{\partial v}{\partial x}\right)^2+\left(\frac{\partial v}{\partial y}\right)^2\right)dA\right\}\\ &\le\iint_\Omega\frac{dV}{dt}\,dA\le0.\end{aligned} \tag{3.9}$$

Therefore, the equilibrium E^* of the spatial system (2.3) is globally asymptotically stable.

4 Existence of Hopf bifurcation around E^*

We analyze the Hopf bifurcation occurring at $E^*(u^*,v^*)$ by choosing ξ as the bifurcation parameter. Also, note that $E^*(u^*,v^*)$ is independent of ξ. The characteristic equation of

system (2.2) at $E^*(u^*, v^*)$ is

$$\lambda^2 - T(\xi)\lambda + D(\xi) = 0. \tag{4.1}$$

The two roots of (4.1) are given as $\lambda = \frac{T \pm \sqrt{T^2 - 4D}}{2} = p_1(\xi) \pm ip_2(\xi)$.

Let $\xi_0 = \left\{ \frac{-r + 2u^* + \frac{\delta(1-m)v^*}{((m-1)u^*(\alpha+(v^*-1)\beta)-1)^2}}{(\zeta - \frac{2v^*}{\eta+(1-m)u^*} - \sigma)} \right\}$. To see the instability of system (2.2), let us state the following theorem.

Theorem 4.1 (*Hopf bifurcation theorem* [28]) *Let $T(\xi)$ and $D(\xi)$ be smooth functions of ξ in an open interval about $\xi_0 \in \mathbb{R}$ such that the characteristic equation has a pair of imaginary eigenvalues $\lambda = p_1(\xi) \pm p_2(\xi)$ with $p_1(\xi)$ and $p_2(\xi) \in \mathbb{R}$ such that λ become purely imaginary at $\xi = \xi_0$ and $\frac{dp_1}{d\xi}|_{\xi=\xi_0} \neq 0$. Then a Hopf bifurcation occurs around E^* at $\xi = \xi_0$ (i.e., stability changes of $E^*(x^*, y^*)$ are accompanied by the formation of a limit cycle when $\xi = \xi_0$).*

Theorem 4.2 *When ξ passes through ξ_0, the local system (2.2) attains a Hopf bifurcation around $E^*(x^*, y^*)$ provided $T(\xi_0) = 0$ and $D(\xi_0) > 0$.*

Proof At $\xi = \xi_0$, the characteristic equation (4.1) becomes

$$\lambda^2 + D(\xi_0) = 0. \tag{4.2}$$

The roots of equation (4.2) are $\lambda_1 = i\sqrt{D(\xi_0)}$ and $\lambda_2 = -i\sqrt{D(\xi_0)}$. Thus, at E^*, two purely imaginary eigenvalues are present. Likewise, $T(\xi)$ and $D(\xi)$ are smooth functions of ξ. Therefore, in the neighborhood of ξ_0, the roots of equation (4.2) are of the form $\lambda_1 = p_1(\xi) + ip_2(\xi)$ and $\lambda_2 = p_1(\xi) - ip_2(\xi)$, where $p_i(\xi)$ are real functions for $i = 1, 2$. Subsequently, let us validate the transversality condition $\frac{d}{d\xi}(\operatorname{Re}\lambda_i(\xi))|_{\xi=\xi_0} \neq 0$, $i = 1, 2$.

By substituting $\lambda(\xi) = p_1(\xi) + ip_2(\xi)$ into the characteristic equation of the Jacobi matrix $J|_{E^*}$ (3.4), we obtain

$$\big(p_1(\xi) + ip_2(\xi)\big)^2 + T\big(p_1(\xi) + ip_2(\xi)\big) + D = 0. \tag{4.3}$$

Differentiating both sides with respect to ξ, we obtain

$$2\big(p_1(\xi) + ip_2(\xi)\big)\big(\dot{p}_1(\xi) + i\dot{p}_2(\xi)\big) + T\big(\dot{p}_1(\xi) + i\dot{p}_2(\xi)\big) + \dot{T}\big(p_1(\xi) + ip_2(\xi)\big) + \dot{D} = 0. \tag{4.4}$$

Collating the real and imaginary parts from both sides, we obtain

$$2p_1(\xi)\dot{p}_1(\xi) - 2p_2(\xi)\dot{p}_2(\xi) + T\big(\dot{p}_1(\xi)\big) + \dot{T}\big(p_1(\xi)\big) + D = 0, \tag{4.5}$$

$$2p_1(\xi)\dot{p}_2(\xi) + 2p_2(\xi)\dot{p}_1(\xi) + T\big(\dot{p}_2(\xi)\big) + \dot{T}\big(p_2(\xi)\big) = 0. \tag{4.6}$$

Equation (4.5) becomes

$$\begin{aligned} &\dot{p}_1(\xi)\big(2p_1(\xi) + T\big) + \dot{p}_2(\xi)\big(-2p_2(\xi)\big) + p_1(\xi)\dot{T} + \dot{D} = 0 \\ &\quad \Longrightarrow \quad \dot{p}_1 B_1 - \dot{p}_2 B_2 + B_3 = 0. \end{aligned} \tag{4.7}$$

Moreover, equation (4.6) becomes

$$\begin{aligned} &\dot{p_1}(\xi)\big(2p_2(\xi)\big) + \dot{p_2}(\xi)\big(2p_1(\xi) + T\big) + p_2(\xi)\dot{T} = 0 \\ &\quad \Longrightarrow \quad \dot{p_1}B_2 + \dot{p_2}B_1 + B_4 = 0, \qquad (4.8) \\ &\text{where } B_1 = \big(2p_1(\xi) + T\big), \qquad B_2 = \big(-2p_2(\xi)\big), \qquad B_3 = p_1(\xi)\dot{T} + \dot{D}, \qquad B_4 = p_2(\xi)\dot{T}. \end{aligned}$$

Multiplying (4.7) by B_1 and (4.8) by B_2 and then adding, we obtain

$$\begin{aligned} &\dot{p_1}\big(B_1^2 + B_2^2\big) + B_1B_3 + B_2B_4 = 0 \\ &\quad \Longrightarrow \quad \dot{p_1} = \frac{-(B_1B_3 + B_2B_4)}{B_1^2 + B_2^2}. \end{aligned}$$

At $\xi = \xi_0$,

Case (i): $p_1 = 0, p_2 = \sqrt{D}$.

$$\begin{aligned} &\text{Then } B_1 = T \neq 0, \qquad B_2 = 2\sqrt{D}, \qquad B_3 = \dot{D}, \qquad B_4 = \dot{T}\sqrt{D}. \\ &\therefore B_1B_3 + B_2B_4 \neq 0 \quad \Longrightarrow \quad \dot{p_1}(\xi)|_{\xi=\xi_0} \neq 0. \end{aligned}$$

Case (ii): $p_1 = 0, p_2 = -\sqrt{D}$.

$$\begin{aligned} &\text{Then } B_1 = T \neq 0, \qquad B_2 = -2\sqrt{D}, \qquad B_3 = \dot{D}, \qquad B_4 = -\dot{T}\sqrt{D}. \\ &\therefore B_1B_3 + B_2B_4 \neq 0 \quad \Longrightarrow \quad \dot{p_1}(\xi)|_{\xi=\xi_0} \neq 0. \end{aligned}$$

□

Theorem 4.3 *Let $D(\xi) > 0$. Then*

(i) *the interior equilibrium point $E^* = (u^*, v^*)$ of system (2.2) is locally asymptotically stable when $\xi > \xi_0$ and unstable when $\xi < \xi_0$; and*

(ii) *the local system (2.2) passes through the Hopf bifurcation at an interior equilibrium $E^* = (u^*, v^*)$ when $\xi = \xi_0$.*

4.1 Stability behavior of Hopf bifurcation

Here, we discuss the behavior of Hopf bifurcation. For this specific purpose, we propose the perturbation $u = u_1 + u_1^{\xi_0}$ and $v = v_1 + v_1^{\xi_0}$ in our local system (2.2). Then, broadening in Taylor series, we obtain

$$\begin{aligned} \dot{u_1} &= a_{10}u_1 + a_{01}v_1 + a_{20}u_1^2 + a_{11}u_1v_1 + a_{30}u_1^3 + a_{21}u_1^2v_1 + \cdots, \\ \dot{v_1} &= b_{10}u_1 + b_{01}v_1 + b_{20}u_1^2 + b_{11}u_1v_1 + b_{30}u_1^3 + b_{21}u_1^2v_1 + \cdots, \end{aligned}$$

where $a_{10} = r - 2u - \frac{\delta(1-m)v}{((m-1)u(\alpha+(v-1)\beta)-1)^2}$, $a_{01} = \frac{\delta(1-m)(-1+(m-1)u(\alpha-\beta))u}{((m-1)u(\alpha+(v-1)\beta)-1)^2}$, $b_{10} = \frac{-\xi_0(m-1)v^2}{(\eta+(1-m)u)^2}$, $b_{01} = \xi_0(\zeta - \frac{2v}{\eta+(1-m)u} - \sigma)$. Therefore, $a_{10} + b_{01} = 0$ and $a_{10}b_{01} - a_{01}b_{10} > 0$.

Various other coefficients are to be determined as given below.

$$\begin{aligned} a_{20} &= 1/2\left(\frac{\partial^2 F}{\partial u^2}\right)\bigg|_{\xi=\xi_0} = -1 - \frac{(m-1)^2v^*(\alpha + (v^* - 1)\beta)\delta}{((m-1)u^*(\alpha + (v^* - 1)\beta) - 1)^3}, \\ a_{11} &= \left(\frac{\partial^2 F}{\partial u \partial v}\right)\bigg|_{\xi=\xi_0} = \frac{(m-1)((m-1)u^*(\alpha - (v^* + 1)\beta) - 1)\delta}{((m-1)u^*(\alpha + (v^* - 1)\beta) - 1)^3}, \end{aligned}$$

$$
\begin{aligned}
a_{30} &= 1/6\left(\frac{\partial^3 F}{\partial u^3}\right)\bigg|_{\xi=\xi_0} = \frac{(m-1)^3 v^*(\alpha+(v^*-1)\beta)^2\delta}{(-1+(m-1)u^*(\alpha+(v^*-1)\beta))^4},\\
a_{21} &= 1/2\left(\frac{\partial^3 F}{\partial u^2 \partial v}\right)\bigg|_{\xi=\xi_0}\\
&= -\Big(\big((m-1)^2(\alpha\big(-1+(m-1)u^*\alpha\big)+\beta-2v^*\beta\\
&\quad -2(m-1)u^*\alpha\beta-(m-1)u^*\big(v^{*2}-1\big)\beta^2)\delta\big)\Big)\\
&\quad \Big/\Big(\big(-1+(m-1)u^*\big(\alpha+\big(v^*-1\big)\beta\big)\big)^4\Big),\\
b_{20} &= 1/2\left(\frac{\partial^2 G}{\partial u^2}\right)\bigg|_{\xi=\xi_0} = \frac{-2(m-1)^2 v^*\xi}{((1-m)u^*+\eta)^3},\\
b_{11} &= \left(\frac{\partial^2 G}{\partial u \partial v}\right)\bigg|_{\xi=\xi_0} = \frac{-2(m-1)v^*\xi}{((1-m)u^*+\eta)^2},\\
b_{30} &= 1/6\left(\frac{\partial^3 G}{\partial u^3}\right)\bigg|_{\xi=\xi_0} = \frac{-(m-1)^3 v^{*2}\xi}{((1-m)u^*+\eta)^4},\\
b_{21} &= 1/2\left(\frac{\partial^3 G}{\partial u^2 \partial v}\right)\bigg|_{\xi=\xi_0} = \frac{-2(1-m)^2 v^*\xi}{((1-m)u^*+\eta)^3},
\end{aligned}
$$

where

$$
\begin{aligned}
F &= u(r-u) - \frac{\delta(1-m)uv}{1+\alpha(1-m)u+\beta((1-m)u)(v-1)},\\
G &= \xi\left(\zeta v - \frac{v^2}{\eta+(1-m)u} - \sigma v\right).
\end{aligned}
$$

By [32], the first Lyapunov number to conclude the dynamics (stable or unstable) of the limit cycle arising through Hopf bifurcation has

$$
\begin{aligned}
\Lambda = {}& \frac{-3\pi}{2a_{01}(a_{10}b_{01}-a_{01}b_{10})^{3/2}}\big(\big[a_{10}b_{10}a_{11}^2 + a_{10}a_{01}\big(b_{11}^2+a_{20}b_{11}\big) - 2a_{10}a_{01}a_{20}^2\\
&- a_{01}^2(2a_{20}b_{20}+b_{11}b_{20}) - \big(a_{01}b_{10}-2a_{10}^2\big)a_{11}a_{20}\big]\\
&- \big(a_{10}^2+a_{01}b_{10}\big)\big[-3a_{01}a_{30}+2a_{10}(a_{21}+b_{12})+(b_{10}a_{12}-a_{01}b_{21})\big]\big).
\end{aligned}
$$

Theorem 4.4 *When $\Lambda < 0$, the direction of Hopf bifurcation is supercritical and the bifurcated periodic solutions are stable; when $\Lambda > 0$, the direction of Hopf bifurcation is subcritical and the bifurcated periodic solutions are unstable.*

5 Diffusion-driven instability

Through this section, we concentrate on the prey–predator system with self-diffusion and examine the occurrence of Turing instability in the equilibrium point under diffusion effects (diffusion-driven instability).

Theorem (4.3) states that whenever $\xi > \xi_0$, the nontrivial interior equilibrium E^* is locally asymptotically stable for the nondiffusion system (2.2).

We consider the influences of diffusion on the stable nontrivial interior equilibrium E^* of (2.3) under the supposition $\xi > \xi_0$. Subsequently, for the diffusion system (2.3), we should

consider the one-dimensional space $\Omega = (0,\pi)$ with a smooth boundary $\partial\Omega$:

$$\begin{aligned} &u_t = u(r-u) - \frac{\delta(1-m)uv}{1+\alpha(1-m)u+\beta((1-m)u)(v-1)} + d_1 u_{xx}, \quad x \in (0,\pi), t > 0, \\ &v_t = \xi\left(\zeta v - \frac{v^2}{\eta+(1-m)u} - \sigma v\right) + d_2 v_{xx}, \quad x \in (0,\pi), t > 0, \\ &u_x(0,t) = u_x(\pi,t) = 0, \qquad v_x(0,t) = v_x(\pi,t) = 0, \quad t > 0. \end{aligned} \tag{5.1}$$

This is actually the notable operator $u \to -u_{xx}$ with Neumann boundary conditions. The analogous eigenvalues and normalized eigenfunctions are

$$\varrho_0 = 0, \qquad \varphi_0(x) = \sqrt{\frac{1}{\pi}}, \qquad \varrho_k = k^2, \qquad \varphi_k(x) = \sqrt{\frac{2}{\pi}}\cos(kx), \quad \text{where } k = 1,2,3,\ldots.$$

Linearizing the above diffusion system (5.1) at E^*, we obtain

$$\begin{bmatrix} u_t \\ v_t \end{bmatrix} = L\begin{bmatrix} u \\ v \end{bmatrix} + J\begin{bmatrix} u \\ v \end{bmatrix} + D\begin{bmatrix} u_{xx} \\ v_{xx} \end{bmatrix},$$

where $D = \operatorname{diag}(d_1, d_2)$ and J is the Jacobian matrix pointed out in Sect. 3.3. L indicates a linear operator whose domain is $D_L = X_{\mathbb{C}} := X \oplus iX = \{u1 + iu2 : u1, u2 \in X\}$, where $X := \{(u,v) \in H^2[(0,\pi)] \times H^2[(0,\pi)] : u_x(0,t) = u_x(\pi,t) = v_x(0,t) = v_x(\pi,t) = 0\}$, which is a real-valued Sobolev space.

Consider the characteristic equation $L(\varphi,\psi)^T = \varrho(\varphi,\psi)^T$, and let

$$(\varphi,\psi)^T = \sum_{k=0}^{\infty}(a_k,b_k)^T\cos(kx). \tag{5.2}$$

Let $J_k = J - k^2 D$. Then we obtain $\sum_{k=0}^{\infty}(J_k - \varrho I)(a_k,b_k)^T\cos(kx) = 0$.

Thus, all eigenvalues of L are obtained by the eigenvalues of J_k for $k = 1,2,3,\ldots$. The characteristic equation of J_k is

$$\varrho^2 - T_k\varrho + D_k = 0, \quad k = 1,2,3,\ldots, \tag{5.3}$$

where

$$\begin{aligned} &T_k = \operatorname{tr} J_k = T - (d_1+d_2)k^2, \\ &\text{and} \quad D_k = \det J_k = D + d_1 d_2 k^4 + (\delta d_1 - \delta_0 d_2)k^2. \end{aligned}$$

Simply by examining the distribution of characteristic roots of J_k, we obtain the imminent conclusion.

Theorem 5.1 *Assume that $\xi > \xi_0$ and $D(\xi) > 0$. Then*

(i) *the equilibrium $E^* = (u^*, v^*)$ of the nondiffused system (2.2) is locally asymptotically stable;*

(ii) *the equilibrium* $E^* = (u^*, v^*)$ *of the diffused system* (5.1) *is locally asymptotically stable if and only if the following conditions hold*:

$$(C1) \quad d_1 \geq \frac{d_2\xi_0}{\xi},$$

$$(C2) \quad d_1 < \frac{d_2\xi_0}{\xi} \quad \textit{and} \quad \frac{d_1}{d_2} > \frac{\xi_0\xi + 2D - 2\sqrt{D(\xi\xi_0 + D)}}{\xi^2}.$$

Furthermore, for the diffused system (5.1), *the solution* E^* *is unstable* (*that is, Turing instability occurs*) *if*

$$(C3) \quad 0 < \frac{d_1}{d_2} < \frac{\xi_0\xi + 2D - 2\sqrt{D(\xi\xi_0 + D)}}{\xi^2} \quad (\textit{Turing instability domain}).$$

Proof Because $\xi > \xi_0$ ($T < 0$) signifies that $T_k < 0$ for all $k \geq 0$. Moreover, by the meaning of T_k, we have the relationship that for every $k \geq 0$, $T_{k+1} < T_k$. We calculate D_k like a quadratic function in k^2, that is, $D_k = D(k^2) = d_1d_2(k^2)^2 + (\xi d_1 - \xi_0 d_2)k^2 + D$. Consequently, the real part of the characteristic values signs of (5.3) are discovered by the sign of $D(k^2)$, separately. The symmetric axis of the graph $(k^2, D(k^2))$ is $k^2_{\min} = -\frac{(\xi d_1 - \xi_0 d_2)}{2d_1d_2}$. We know that when $D_k < 0$ ($D(k^2) < 0$), the characteristic roots of J_k (5.3) are two real roots with opposite signs. Notice that in $D(k^2)$, $d_1d_2 > 0$ and $k^2 > 0$. Therefore, whenever $\xi d_1 - \xi_0 d_2 < 0$, $D(k^2)$ attains the bare minimum at $k^2 = k^2_{\min}$.

Therefore, when $(C3)$ holds, $D(k^2_{\min})$ is negative. However, this means that any one of the characteristic roots of J_k have a positive real part, that is, that E^* is the unstable solution of (5.1). As a result, we consider that whenever $(C3)$ holds, Turing instability occurs. $(C1)$ implies that $D_k > 0$ for all $k \geq 0$ (because $D_0 = D > 0$), and $(C2)$ implies that $D(k^2_{\min})$ is positive, and therefore that all the characteristic roots of J_k have negative real parts. In this manner, any of conditions $(C1)$ and $(C2)$ guarantee that the characteristic roots of J_k have negative real parts. Consequently, if any one of the conditions of $(C1)$ and $(C2)$ holds, then E^* is the stable equilibrium solution of (5.1). □

6 Numerical simulation

In this section, we describe a few numerical simulations performed to verify our analytical findings using MATLAB. We consider system (2.2) with fixed parameters $\{r = 0.7, \delta = 1.5, \alpha = 0.8, \beta = 0.4, \xi = 1.8, \zeta = 1.7, \eta = 0.4, \sigma = 1.4, 0 \leq m = 0.35 < 1\}$. For these parametric values, the corresponding nullclines are shown in Fig. 1. The pink and orange curves represent the prey and predator nullclines, respectively. Intersecting points of nullclines are given by equilibrium points E_0, E_1, E_2, and $E^*(u^*, v^*) = (0.51525, 0.22047)$. Note that, for the above set of parameters, one condition $\Delta_3 > 0$ is violated in (H) although there exists a unique E^* in $\mathbb{R}^2_+$. Therefore, the set of conditions we mentioned in (H) is necessary but not sufficient for the existence and uniqueness of $E^* \in \mathbb{R}^2_+$.

Through the vector fields (blue arrows) in Fig. 1, we may understand the stability of the equilibriums. For this set of parameters, $E_0 = (0, 0)$ is unstable. In particular, for this case, E_0 is a nodal source. Also, where $\zeta = 1.7 > \sigma = 1.4$, therefore $E_1 = (r, 0) = (1.7, 0)$ and $E_2 = (0, \zeta\eta - \eta\sigma) = (0, 0.12)$ are also unstable (saddle points).

By fixing the same set of above parameters other than ζ and σ with condition $\zeta = 1.4 < \sigma = 1.7$, our resultant phase plane is shown in Fig. 2. Because $\zeta < \sigma$, the axial equilibrium

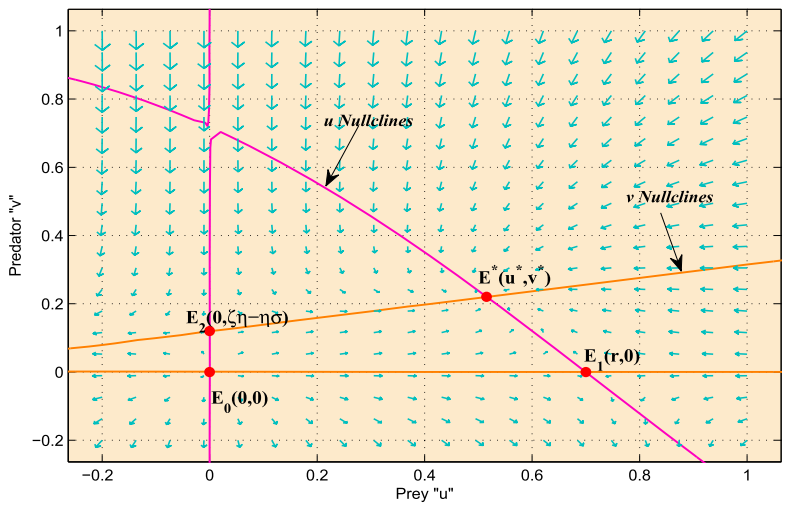

Figure 1 Nullclines of a prey–predator system (2.2) with parameters $\{r = 0.7, \delta = 1.5, \alpha = 0.8, \beta = 0.4, \xi = 1.8, \zeta = 1.7, \eta = 0.4, \sigma = 1.4, m = 0.35\}$

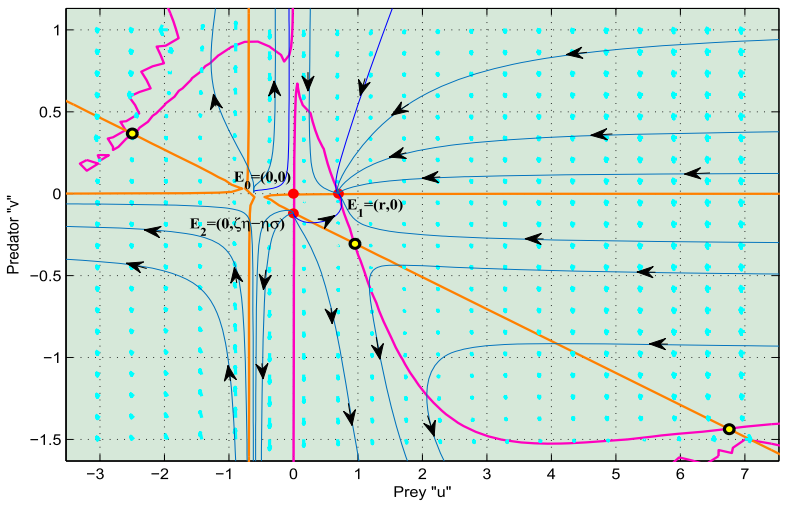

Figure 2 Phase plane of the prey–predator system (2.2) with parameters $\{r = 0.7, \delta = 1.5, \alpha = 0.8, \beta = 0.4, \xi = 1.8, \zeta = 1.4, \eta = 0.4, \sigma = 1.7, m = 0.35\}$

$E_2 = (0, \zeta\eta - \eta\sigma) = (0, -0.12) \notin \{\{0\} \cup \mathbb{R}\}^2_+$. We drew different phase trajectories starting from various initial points. From the phase plane, we obtain that $E_1 = (r, 0) = (0.7, 0)$ is locally asymptotically stable (a nodal sink). Also, Fig. 2 shows that E_0 is unstable (a saddle point) and E_2 is unstable (a nodal source). Also note that for this set of parametric values, the conditions $\Delta_1 < 0$, $\Delta_3 > 0$ do not hold in (H). Therefore, no interior equilibrium $E^*(u^*, v^*)$ exists in $\mathbb{R}^2_+$. However, there were three nontrivial equilibriums (yellow dots) on quadrants II and III of the phase plane. From the biological perspective, these are meaningless. The following set possesses all conditions of (H) and $\zeta > \sigma$: $\{r = 1, \delta = 0.8, \alpha = 10, \beta = 0.1, \xi = 0.15, \zeta = 7.1, \eta = 0.01, \sigma = 6, 0 \le m = 0.01 < 1\}$. Then there exists a unique nontrivial interior equilibrium $E^*(u^*, v^*) = (0.920642, 1.01358) \in \mathbb{R}^2_+$, which is shown in Fig. 3. For these parameter values, the trivial equilibrium point $E_0 = (0, 0)$ is unstable and axial equi-

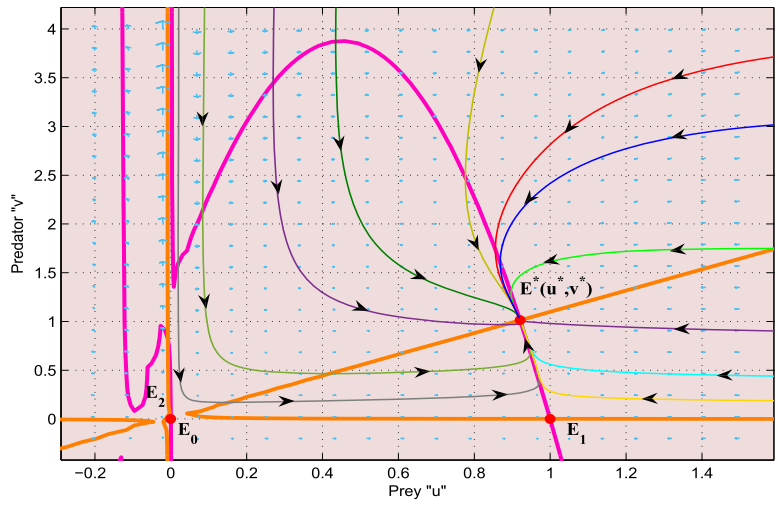

Figure 3 Existence and uniqueness of $E^*(u^*, v^*)$. The parametric values are taken as $\{r = 1, \delta = 0.8, \alpha = 10, \beta = 0.1, \xi = 0.15, \zeta = 7.1, \eta = 0.01, \sigma = 6, m = 0.01\}$. Moreover, the steady state $E^* = (0.920642, 1.01358)$ is globally asymptotically stable. Because $(\delta(1-m)v^* - u^*)\alpha < \frac{1}{1-m} + \beta u^*(v^* - 1)$ and $(1-m)u^*(\beta - \alpha) < 1$

librium $E_1 = (1, 0)$ and $E_2 = (0, 0.011)$ are saddle points. Further, the above set of parameters follows the conditions $(\delta(1-m)v^* - u^*)\alpha < \frac{1}{1-m} + \beta u^*(v^* - 1)$ and $(1-m)u^*(\beta - \alpha) < 1$. As per Theorem 3.2, Fig. 3 shows that different phase trajectories start from different initial points, but ultimately all the trajectories converge to the same interior equilibrium point $E^* = (0.920642, 1.01358)$. This shows that E^* is globally asymptotically stable.

Now, consider the prey–predator model (2.2) together with the following set of parameters: $\{r = 1, \delta = 8, \alpha = 10, \beta = 0.1, \zeta = 7.1, \eta = 0.01, \sigma = 6, m = 0.01\}$. Then our ODE model becomes

$$\begin{cases} \frac{du}{dt} = u(1-u) - \frac{8(1-0.01)uv}{1+10(1-0.01)u+0.1((1-0.01)u)(v-1)}, \\ \frac{dv}{dt} = \xi(7.1v - \frac{v^2}{0.01+(1-0.01)u} - 6v), \\ u(0) = u_0 > 0, \qquad v(0) = v_0 > 0. \end{cases} \tag{6.1}$$

Under this set of parameters, the above system (6.1) has a unique nontrivial positive interior equilibrium $E^*(u^*, v^*) = (0.315572, 0.3554658)$. Pertaining to the preceding parametric values, the crucial point value is $\xi_0 = 0.183713$, which is independent of ξ. Further, we vary the bifurcation parameter ξ only.

By fixing $\xi = 0.2$, we obtain $\xi > \xi_0 = 0.183713$, and it follows from Theorem (4.3) that $E^*(u^*, v^*)$ is locally asymptotically stable (see Fig. 4).

Fixing $\xi = \xi_0 = 0.183713$ implies that $T(\xi_0) = 0$. Subsequently, by Theorem (4.3), E^* loses its stability and a Hopf bifurcation arises, that is, a family group of intermittent periodic solutions bifurcating from the interior equilibrium E^* (see Fig. 5).

Through $\xi = 0.15$, we certainly have $\xi < \xi_0$, and it follows by Theorem (4.3) that $E^*(u^*, v^*)$ is unstable (see Fig. 6).

Moreover, when ξ goes through ξ_0 from the right-hand side of ξ_0, the equilibrium point E^* loses its steadiness and a Hopf bifurcation occurs, as shown in Fig. 5 and Fig. 6. For the above set of parameters, we obtain $\Lambda = -9.01885 < 0$. Therefore, from Theorem 4.4,

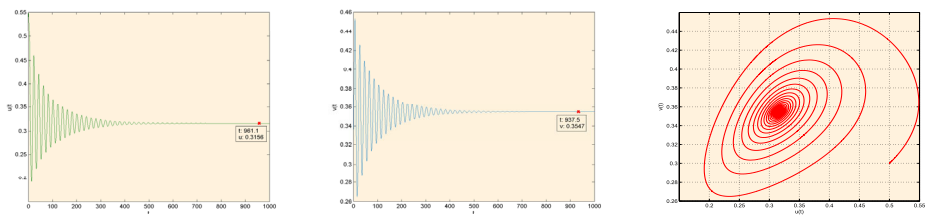

Figure 4 Stability behavior with respect to time t and phase portraits of system (2.2) with $\xi > \xi_0$ and initial data $(u_0, v_0) = (0.5, 0.3)$

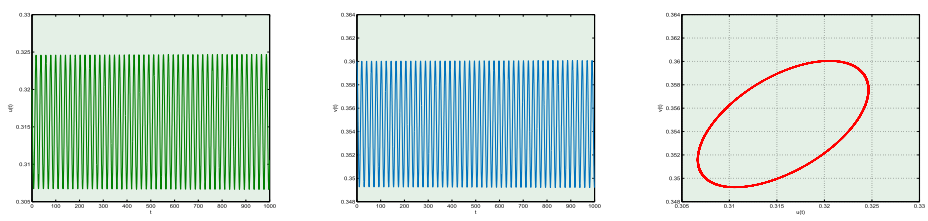

Figure 5 Periodic behavior with respect to time t and phase portraits of system (2.2) with $\xi = \xi_0$ and initial data $(u_0, v_0) = (0.32, 0.36)$

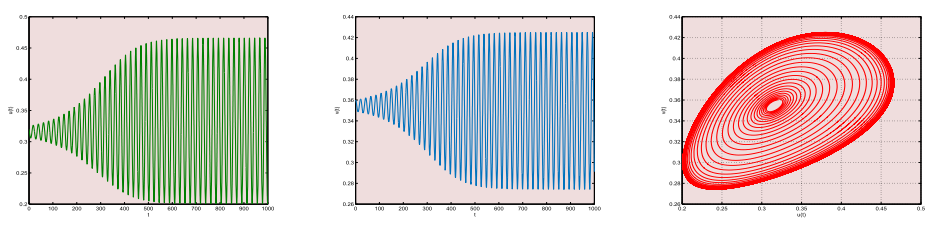

Figure 6 Unstable behavior with respect to time t and phase portraits of system (2.2) with $\xi < \xi_0$ and initial data $(u_0, v_0) = (0.32, 0.36)$

the direction of the Hopf bifurcation at $\xi = \xi_0$ is supercritical, and the bifurcating periodic solutions are asymptotically stable, as shown in phase diagrams of Fig. 5 and Fig. 6.

The formation of a limit cycle around the interior equilibrium point with initial data $(0.4, 0.3)$ and $(0.5, 0.5)$ inside and outside of the limit cycle, respectively, is shown in Fig. 7. The diagram shows that the limit cycle is stable.

To verify the occurrence of Turing instability of the diffusive prey–predator system (5.1), we consider the following set with Neumann boundary condition on a one-dimensional spatial domain $\Omega = (0, 60)$: $\{r = 1, \delta = 8, \alpha = 10, \beta = 0.1, \zeta = 7.1, \eta = 0.01, \sigma = 6, m = 0.01\}$. We modify the diffusion coefficients d_1 and d_2 only.

Within the parameters $d_1 = 1$, $d_2 = 2$ and $\xi = 0.2$ $(0.2 = \xi > \xi_0 = 0.183713)$, also $1 = d_1 < \frac{d_2\xi_0}{\xi} = 1.83713$ and $\frac{d_1}{d_2} = 0.5 > \frac{\xi_0\xi + 2D - 2\sqrt{D(\xi\xi_0 + D)}}{\xi^2} = 0.071$, that is, (C2) holds. By Theorem 5.1, the homogeneous equilibrium solution E^* of system (5.1) is stable. The stability behavior and the corresponding contour diagram is shown in Fig. 8.

Under the parameters $d_1 = 0.01$, $d_2 = 1$ and $\xi = 0.2$ $(\xi > \xi_0)$, $0.01 = \frac{d_1}{d_2} < \frac{\xi_0\xi + 2D - 2\sqrt{D(\xi\xi_0 + D)}}{\xi^2} = 0.071$, that is, (C3) holds. By Theorem 5.1, the homogeneous equilib-

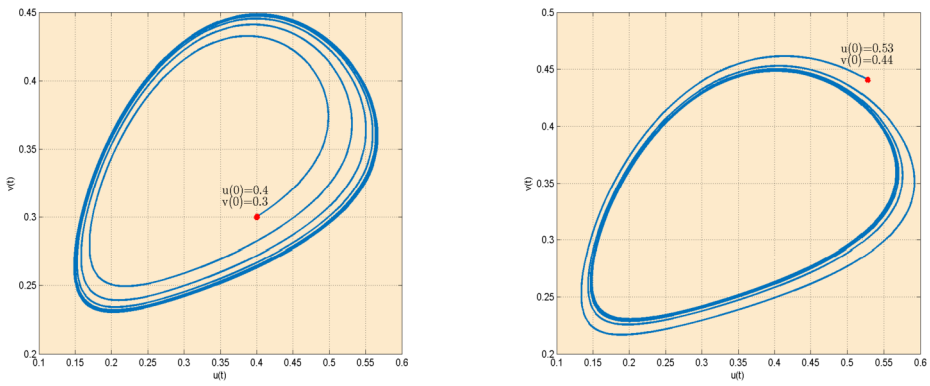

Figure 7 Existence of a stable limit cycle around the interior equilibrium $E^* = (0.315572, 0.354658)$

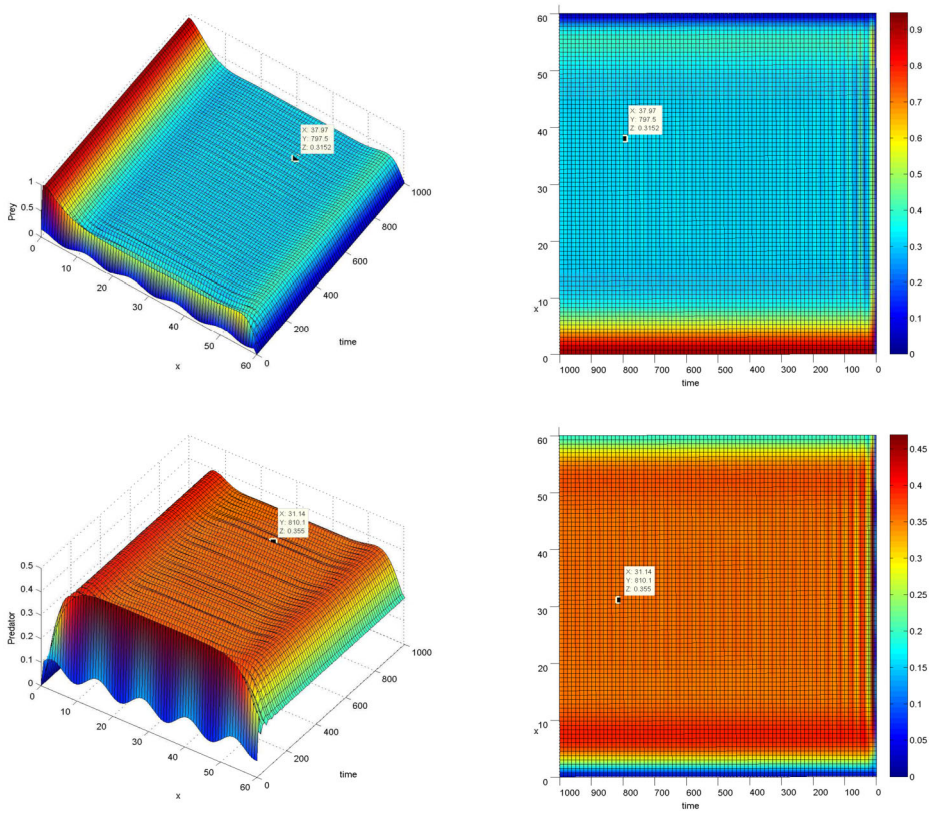

Figure 8 Numerical simulations of the diffusion system (5.1) with parameter restriction $\xi = 0.2$ ($0.2 = \xi > \xi_0 = 0.183713$), $d_1 = 1$ and $d_2 = 2$, with the initial condition ($t = 0$, $0.1 + 0.05(\cos(\frac{1}{2}u))$, $0.1 + 0.03\sin(\frac{1}{2}v)$)

rium solution E^* of system (5.1) is unstable. That is, Turing instability occurs. The Turing instability and the corresponding contour diagram are shown in Fig. 9.

7 Conclusion

Our study focused on investigating the dynamic behavior of a prey–predator model that incorporates prey refuge and interference among predators. The interaction between prey

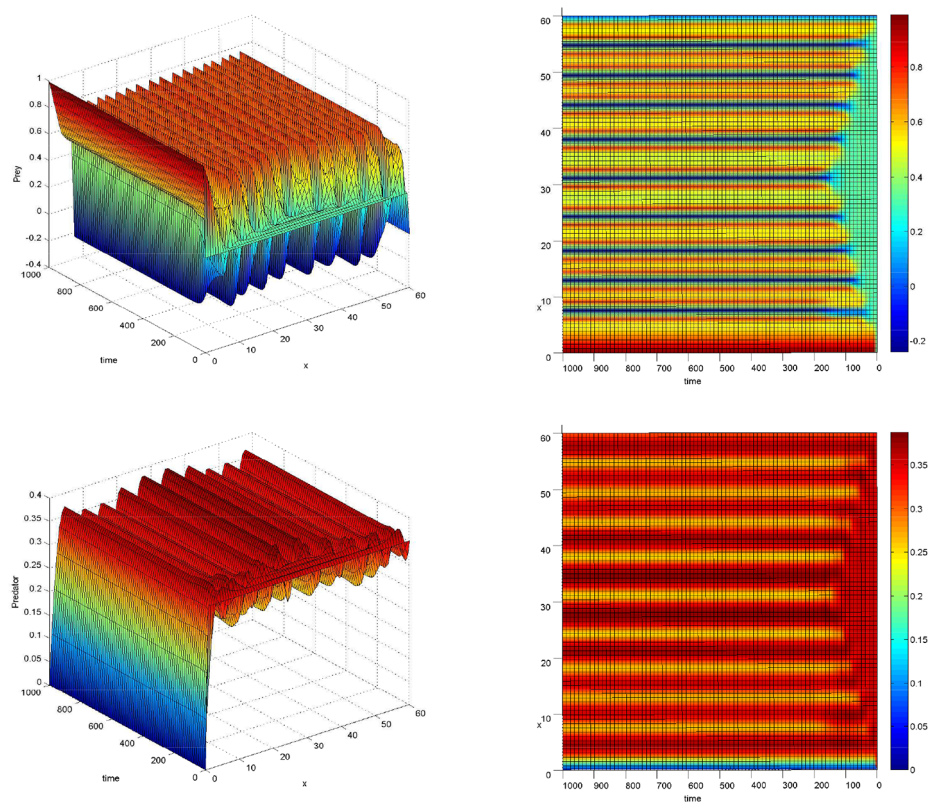

Figure 9 Numerical simulations of the diffusion system (5.1) with parameter restriction $\xi = 0.2$ ($0.2 = \xi > \xi_0 = 0.183713$), $d_1 = 0.01$ and $d_2 = 1$, with the initial condition ($t = 0, 0.31, 0.35$)

and predators was governed by the Crowley–Martin response function. Our key contribution lies in the thorough analysis of the refuge function during intraspecific competition among predators for prey.

Throughout our investigation, we successfully established the existence criteria for biologically meaningful axial and interior equilibrium points, and we assessed their stability. Particularly, we found that when the growth rate of predators, based on the conversion coefficients from individual prey to individual predators, exceeds the death rate of predators ($\zeta = r_2\rho/\delta_2 > \sigma = \delta_3\rho/\delta_2$), only predators will survive ($v^* > 0$).

Moreover, we identified the influential role of the parameter ξ, independent of E^*, in causing a Hopf bifurcation around E^*. Theorem 4.3 reveals that when $D > 0$ and the proportion between the maximal per capita predator consumption rate and the intensity of competition among individuals of the prey species ($\xi = \delta_2/\rho$) exceeds the critical value ξ_0, the prey–predator inhabitants are stable for any initial interior population. This emphasizes the significance of prey refuge and interference among predators in maintaining stable populations. However, when the ratio between the maximal per capita predator consumption rate and the intensity of competition among individuals of the prey species falls below the critical value ξ_0, the population size becomes unstable and cannot be precisely determined. When this ratio precisely equals the critical value ξ_0, the prey–predator inhabitant dynamics exhibit periodic changes due to the occurrence of Hopf bifurcation, as presented in Theorem 4.4.

Furthermore, we delved into the dynamics of the prey–predator population, considering both spatial and temporal motion. To capture spatial movements, we analyzed a diffusion system (5.1) and explored the diffusion-driven instability of the spatial system in detail. We observed that the stability of the interior equilibria E^* could vary from stable to unstable, even when $\xi > \xi_0$ was satisfied due to the occurrence of diffusion-driven effects. The corresponding results are presented in Theorem 5.1. To validate our analytical findings, we provided numerical examples in Sect. 6, ensuring the robustness of our results.

As we conclude our study, we recognize that an exciting avenue for future research would involve exploring the impact of stochastic noise on the model, particularly in terms of habitat-dependent parameters. Incorporating stochastic elements could offer valuable insights into the system's resilience and adaptability under varying environmental conditions.

In summary, our work contributes to a deeper understanding of the complex dynamics within prey–predator ecosystems, shedding light on how refuge and interactions among predators play pivotal roles in governing population stability and behavior. Our findings open the door to further investigations and offer potential applications in ecological management and conservation efforts.

Funding
The work of Yong-Ki Ma was supported by the National Research Foundation of Korea (NRF) grant funded by the Korea government (MSIT) (No. 2021R1F1A1048937).

Availability of data and materials
This study contains numerical experimental results, and the values of these experiments are included in the work. The data are freely available.

Code availability
The values of these experiments are freely available.

Declarations

Ethics approval and consent to participate
Not applicable.

Competing interests
The authors declare no competing interests.

Author contributions
All the authors have contributed equally to this paper. All authors read and approved the final revised manuscript.

Author details
[1]Department of Mathematics, B V Raju Institute of Technology, Narsapur, Medak, Telangana 502 313, India. [2]Department of Mathematics, Periyar University, Salem 636 011, India. [3]Department of Mathematics, Bharathiar University, Coimbatore 641 046, India. [4]Department of Applied Mathematics, Kongju National University, Gongju-si, Chungcheongnam-do 32588, Republic of Korea.

Received: 22 June 2023 Accepted: 30 July 2023 Published online: 16 August 2023

References

1. Bazykin, A.D.: Nonlinear Dynamics of Interacting Populations. World Scientific, Singapore (1998)
2. Beddington, J.R.: Mutual interference between parasites or predators and its effect on searching efficiency. J. Anim. Ecol. **44**, 331–340 (1975)
3. Belabbas, M., Ouahab, A., Souna, F.: Rich dynamics in a stochastic predator-prey model with protection zone for the prey and multiplicative noise applied on both species. Nonlinear Dyn. **106**, 2761–2780 (2021)
4. Braza, P.A.: The bifurcation structure of the Holling-Tanner model for predator-prey interactions using two-timing. SIAM J. Appl. Math. **63**, 889–904 (2003)
5. Cantrell, R.S., Cosner, C.: On the dynamics of predator-prey models with the Beddington-DeAngelis functional response. J. Math. Anal. Appl. **257**, 206–222 (2001)
6. Cao, X., Jiang, W.: Turing-Hopf bifurcation and spatiotemporal patterns in a diffusive predator-prey system with Crowley-Martin functional response. Nonlinear Anal., Real World Appl. **43**, 428–450 (2018)

7. Celik, C.: Stability and Hopf bifurcation in a delayed ratio dependent Holling-Tanner type model. Appl. Math. Comput. **255**, 228–237 (2015)
8. Chen, S., Shi, J.: Global stability in a diffusive Holling-Tanner predator-prey model. Appl. Math. Lett. **25**, 614–618 (2012)
9. Collings, J.B.: Bifurcation and stability analysis of a temperature-dependent mite predator-prey interaction model incorporating a prey refuge. Bull. Math. Biol. **57**, 63–76 (1995)
10. Crowley, P.H., Martin, E.K.: Functional responses and interference within and between year classes of a dragonfly population. J. North Am. Benthol. Soc. **8**, 211–221 (1989)
11. DeAngelis, D.L., Goldstein, R.A., O'Neill, R.V.: A model for tropic interaction. Ecology **56**, 881–892 (1975)
12. Ghosh, J., Sahoo, B., Poria, S.: Prey-predator dynamics with prey refuge providing additional food to predator. Chaos Solitons Fractals **96**, 110–119 (2017)
13. Goh, B.S.: Global stability in two-species interactions. J. Math. Biol. **3**, 313–318 (1976)
14. Gokila, C., Sambath, M., Balachandran, K., Ma, Y.-K.: Analysis of stochastic predator-prey model with disease in the prey and Holling type II functional response. Adv. Math. Phys. **2020**, 3632091 (2020)
15. Guin, L.N., Pal, S., Chakravarty, S., Djilali, S.: Pattern dynamics of a reaction-diffusion predator-prey system with both refuge and harvesting. Int. J. Biomath. **40**, 2050084 (2020)
16. Hassell, M.P.: The Dynamics of Arthropod Predator-Prey Systems. Princeton University Press, Princeton (1978)
17. Hassell, M.P., May, R.M.: Stability in insect host-parasite models. J. Anim. Ecol. **42**, 693–726 (1973)
18. Holling, C.S.: The functional response of predators to prey density and its role in mimicry and population regulation. Mem. Entomol. Soc. Can. **97**, 5–60 (1965)
19. Hsu, S.B., Huang, T.W.: Hopf bifurcation analysis for a predator-prey system of Holling and Leslie type. Taiwan. J. Math. **3**, 35–53 (1999)
20. Hsu, S.B., Hwang, T.W.: Global stability for a class of predator-prey systems. SIAM J. Appl. Math. **55**, 763–783 (1995)
21. Krivan, V.: Effects of optimal antipredator behavior of prey on predator-prey dynamics: the role of refuges. Theor. Popul. Biol. **53**, 131–142 (1998)
22. Li, X., Jiang, W., Shi, J.: Hopf bifurcation and Turing instability in the reaction-diffusion Holling-Tanner predator-prey model. IMA J. Appl. Math. **76**, 1–20 (2011)
23. Liu, P.P., Xue, Y.: Spatiotemporal dynamics of a predator-prey model. Nonlinear Dyn. **69**, 71–77 (2012)
24. Ma, Z.P., Li, W.T.: Bifurcation analysis on a diffusive Holling-Tanner predator-prey model. Appl. Math. Model. **37**, 4371–4384 (2013)
25. Mondal, S., Samanta, G.P.: Dynamics of an additional food provided predator-prey system with prey refuge dependent on both species and constant harvest in predator. Phys. A, Stat. Mech. Appl. **534**, 122301 (2019)
26. Mondal, S., Samanta, G.P.: Provision of additional food as a tool of biological control in a delayed predator-prey interaction with prey refuge. Int. J. Model. Simul. **42**, 570–594 (2022)
27. Mougi, A.: Predator interference and complexity-stability in food webs. Sci. Rep. **12**, 1–8 (2022)
28. Murray, J.D.: Mathematical Biology-I: An Introduction. Springer, Berlin (2007)
29. Papanikolaou, N.E., Dervisoglou, S., Fantinou, A., Kypraios, T., Giakoumaki, V., Perdikis, D.: Predator size affects the intensity of mutual interference in a predatory mirid. Ecol. Evol. **11**, 1342–1351 (2021)
30. Peng, R., Wang, M.: Global stability of the equilibrium of a diffusive Holling-Tanner prey-predator model. Appl. Math. Lett. **20**, 664–670 (2007)
31. Peng, R., Wang, M.: Stationary patterns of the Holling-Tanner prey-predator model with diffusion and cross-diffusion. Appl. Math. Comput. **196**, 570–577 (2008)
32. Perko, L.: Differential Equations and Dynamical Systems. Springer, Berlin (2013)
33. Rosenzweig, M.L., MacArthur, R.H.: Graphical representation and stability conditions of predator-prey interactions. Am. Nat. **97**, 209–223 (1963)
34. Saha, S., Samanta, G.P.: Analysis of a predator-prey model with herd behavior and disease in prey incorporating prey refuge. Int. J. Biomath. **12**, 1950007 (2019)
35. Sambath, M., Balachandran, K.: Bifurcations in a diffusive predator-prey model with predator saturation and competition response. Math. Methods Appl. Sci. **38**, 785–798 (2015)
36. Sen, M., Banerjee, M., Morozov, A.: Bifurcation analysis of a ratio-dependent prey-predator model with the Allee effect. Ecol. Complex. **11**, 12–27 (2012)
37. Sharma, S., Samanta, G.P.: A Leslie-Gower predator-prey model with disease in prey incorporating a prey refuge. Chaos Solitons Fractals **70**, 69–84 (2015)
38. Skalski, G.T., Gilliam, J.F.: Functional responses with predator interference: viable alternatives to the Holling type II model. Ecology **82**, 3083–3092 (2001)
39. Souna, F., Belabbas, M., Menacer, Y.: Complex pattern formations induced by the presence of cross-diffusion in a generalized predator–prey model incorporating the Holling type functional response and generalization of habitat complexity effect. Math. Comput. Simul. **204**, 597–618 (2023)
40. Souna, F., Djilali, S., Charif, F.: Mathematical analysis of a diffusive predator-prey model with herd behavior and prey escaping. Math. Model. Nat. Phenom. **15**, 23 (2020)
41. Souna, F., Lakmeche, A.: Spatiotemporal patterns in a diffusive predator–prey system with Leslie-Gower term and social behavior for the prey. Math. Methods Appl. Sci. **44**, 13920–13944 (2021)
42. Souna, F., Lakmeche, A., Djilali, S.: Spatiotemporal patterns in a diffusive predator-prey model with protection zone and predator harvesting. Chaos Solitons Fractals **140**, 110180 (2020)
43. Souna, F., Tiwari, P.K., Belabbas, M., Menacer, Y.: A predator–prey system with prey social behavior and generalized Holling III functional response: role of predator-taxis on spatial patterns. Math. Methods Appl. Sci. (2023)
44. Surendar, M.S., Sambath, M.: Modeling and numerical simulations for a prey-predator model with interference among predators. Int. J. Model. Simul. Sci. Comput. **12**, 2050065 (2021)
45. Surendar, M.S., Sambath, M., Balachandran, K.: Bifurcation on diffusive Holling Tanner predator-prey model with stoichiometric density dependence. Nonlinear Anal., Model. Control **25**, 225–244 (2020)
46. Tang, X., Jiang, H., Deng, Z., Yu, T.: Delay induced subcritical Hopf bifurcation in a diffusive predator-prey model with herd behavior and hyperbolic mortality. J. Appl. Anal. Comput. **7**, 1385–1401 (2017)
47. Tiwari, B., Raw, S.N.: Dynamics of Leslie-Gower model with double Allee effect on prey and mutual interference among predators. Nonlinear Dyn. **103**, 1229–1257 (2021)

48. Tripathi, J.P., Jana, D., Devi, N.V., Tiwari, V., Abbas, S.: Intraspecific competition of predator for prey with variable rates in protected areas. Nonlinear Dyn. **102**, 511–535 (2020)
49. Xiao, D., Ruan, S.: Global analysis in a predator-prey system with nonmonotonic functional response. SIAM J. Appl. Math. **61**, 1445–1472 (2001)
50. Zhu, H., Campbell, S.A., Wolkowicz, G.S.: Bifurcation analysis of a predator-prey system with nonmonotonic functional response. SIAM J. Appl. Math. **63**, 636–682 (2003)

Publisher's Note

Springer Nature remains neutral with regard to jurisdictional claims in published maps and institutional affiliations.

Submit your manuscript to a SpringerOpen journal and benefit from:

- ► Convenient online submission
- ► Rigorous peer review
- ► Open access: articles freely available online
- ► High visibility within the field
- ► Retaining the copyright to your article

Submit your next manuscript at ► springeropen.com